AIMS Materials Science, 9(1): 105–118.
DOI: 10.3934/matersci.2022007
Received: 14 September 2021
Revised: 22 December 2021
Accepted: 27 December 2021
Published: 12 January 2022

http://www.aimspress.com/journal/Materials

Research article

Investigation of ZnO doping on $LaFeO_3/Fe_2O_3$ prepared from yarosite mineral extraction for ethanol gas sensor applications

Endi Suhendi[1,*], Andini Eka Putri[1], Muhamad Taufik Ulhakim[1], Andhy Setiawan[1] and Dani Gustaman Syarif[2]

[1] Physics Study Program, Universitas Pendidikan Indonesia, Bandung, Indonesia
[2] Center of Science and Technology of Applied Nuclear, National Nuclear Energy Agency of Indonesia (BATAN), Bandung, Indonesia

* **Correspondence:** Email: endis@upi.edu.

Abstract: In this study, we used a natural resource, yarosite minerals, as a Fe_2O_3 precursor. Yarosite minerals were used for the synthesis of $LaFeO_3/Fe_2O_3$ doped with ZnO via a co-precipitation method using ammonium hydroxide, which produced a light brown powder. Then, an ethanol gas sensor was prepared using a screen-printing technique and characterized using gas chamber tools at 100, 200, and 300 ppm of ethanol gas to investigate the sensor's performance. Several factors that substantiate electrical properties such as crystal and morphological structures were also studied using X-Ray Diffraction (XRD) and Scanning Electron Microscopy (SEM), respectively. The crystallite size decreased from about 61.4 nm to 28.8 nm after 0.5 mol% ZnO was added. The SEM characterization images informed that the modified $LaFeO_3$ was relatively the same but not uniform. Lastly, the sensor's electrical properties exhibited a high response of about 257% to 309% at an operating temperature that decreased from 205 ℃ to 180 ℃. This finding showed that these natural resources have the potential to be applied in the development of ethanol gas sensors in the future. Hence, yarosite minerals can be considered a good natural resource that can be further explored to produce an ethanol gas sensor with more sensitive response. In addition, this method reduces the cost of material purchase.

Keywords: $LaFeO_3/Fe_2O_3$; ZnO; yarosite minerals; ethanol gas sensors

1. Introduction

Many researchers are currently deliberating about gas sensors, focusing on the development of metal oxide semiconductor (MOS) gas-sensing due to its potential applications in the technology industry to monitor safety. Apart from that, it can also be employed in daily life to monitor health processes [1]. As a gas sensing material, the MOS has been developed in various forms [2], one of which is the modification of gas-sensing material by several researchers to obtain high-performance gas sensors [3–7]. Generally, MOSs have been used to detect harmful gases such as formaldehyde [8], toluene [9], NO_2 [10], acetone [11], and ethanol [12]. Among these gases, ethanol is more widely used in daily life products, such as the food and medicine industries [13]. Ethanol easily evaporates in the air and poses considerable risks [14]. Hence, in order to ensure safety, it is crucial to develop ethanol gas sensors to monitor industrial processes.

To this date, ethanol gas sensors have been developed with various types of MOSs such as SnO_2 [15], WO_3 [16], Fe_2O_3 [17], and $LaFeO_3$ [18]. MOS can be divided into two groups: n-type and p-type. The p-type semiconductor responds better to ethanol gases because they have excellent catalytic activity and significantly higher oxygen ion mobility [19]. The p-type semiconductor material that has been applied extensively in many ethanol gas sensors is $LaFeO_3$ due to its high stability and tunability [20]. In addition, considerable effort has been devoted to using $LaFeO_3$ as an ethanol-gas-sensing material due to its high resistance [21]. Also, $LaFeO_3$ were chosen due to their good characteristics in oxidation or reduction and significant sensitive to reducing gases, such as ethanol [22].

As previously mentioned, a method of solving these problems is to modify gas-sensing materials, and in this case, by doping $LaFeO_3$. Doping can reduce the resistance of $LaFeO_3$ [23]. Doping is used to influence the crystal structure, morphology, and electrical properties of the material to optimize the performance of gas sensors [24], including $LaFeO_3$-based ethanol gas sensors. Many researchers have applied this treatment and added some doping to $LaFeO_3$ using various elements such as Mg [25], Zn [26], Ag [26,27], Cr [28], and Co [28,29]. Among these elements, Zn is rarely used even though it provides a better response in ethanol gas sensors; it was used by Chen et al. [26], who reported that Zn doping plays an important role because it can reduce the resistance even by small amounts. In addition, the presence of Zn increases the response to ethanol gases. Zn doping affects Fe^{2+} ions, creating oxygen vacancies and increasing the amount of electron hopping of Fe^{3+}–Fe^{2+} [30]. These processes can increase the gas-sensing properties of the materials, such as the electrical properties, i.e., the response and operating temperature [31]. This shows that the influence of doping of gas-sensing material is a topic requiring further study. The $LaFeO_3/Fe_2O_3$ co-doped Ca and Zn was synthesized, and found that the gas sensor performance, especially the response to detecting ethanol, had significantly improved. The response to ethanol gases increased by about 41% compared to $LaFeO_3/Fe2O_3$ without doping [32], demonstrating the potential for applying doping for improving gas sensor performance.

Based on the above, in this study, $LaFeO_3$ modified with the addition of 0.5 mol% ZnO was synthesized for application in ethanol gas sensing based thick film that was fabricated using screen printing. The dose of 0.5 mol% ZnO doping was chosen based on the previous studies from Lai et al. [33] that using the composition of ZnO with the amount of 0.5 mol% and exhibited a good characteristics to applied as gas sensing application. Hence, in this research we used 0.5 mol% for the dosage of ZnO doping to establish the performance of $LaFeO_3/Fe_2O_3$ will do better as the previous work or worse. Then, screen printing is a technology that is commonly used for thick-film fabrication, and it can produce multiple layers of the thick film [34]. The advantages of applying screen

printing for gas sensing is its low cost and the easy deposition of thick-film layers [35,36]. However, a large deposition affects the gas sensor's performance. The proposed ethanol gas sensor based on modified $LaFeO_3/Fe_2O_3$ with the addition of 0.5 mol% ZnO is characterized using X-Ray Diffraction (XRD), Scanning Electron Microscopy (SEM), and electrical properties to determine its performance.

2. Materials and methods

2.1. Chemicals

Extracted and purified yarosite minerals were used as the ferric oxide (Fe_2O_3) precursor in the preparation of $LaFeO_3/Fe_2O_3$ doped with 0.5 mol% ZnO powders. The other chemicals, i.e., lanthanum chloride heptahydrate ($LaCl_3 \cdot 7H_2O$), zinc sulfate ($ZnSO_4$), hydrochloric acid (HCl) 2.0 M, distilled water, and ammonium hydroxide (NH_4OH), were of analytical grade. Then, the thick film ceramics were prepared using alumina substrate, silver paste (Ag), ethyl cellulose, and alpha-terpineol. For ethanol detection, we used 97% ethanol as the target.

2.2. Synthesized $LaFeO_3$-Fe_2O_3 doped with ZnO powders

The $LaFeO_3/Fe_2O_3$ doped with 0.5 mol% ZnO powders is synthesized using the co-precipitation method, as illustrated in Figure 1. Firstly, 50 mol% $LaCl_3 \cdot 7H_2O$ is dissolved in the distilled water. Then 49.5 mol% Fe_2O_3 and 0.5 mol% $ZnSO_4$ are dissolved in the 2.0 M HCl, separately, with a magnetic stirrer at room temperature. Afterwards, each solution is produced by simultaneously mixing and stirring until it becomes homogeneous. Next, NH_4OH is slowly added until the solution reaches pH = 7 and it is then left for 12 h. Next, the precipitate is filtered and dried at 100 ℃ for 6 h. Lastly, the product is calcined at 800 ℃ for 6 h until the brown light powders are produced. This experiment also synthesizes the dark brown powders of $LaFeO_3/Fe_2O_3$ using the same treatment for comparison.

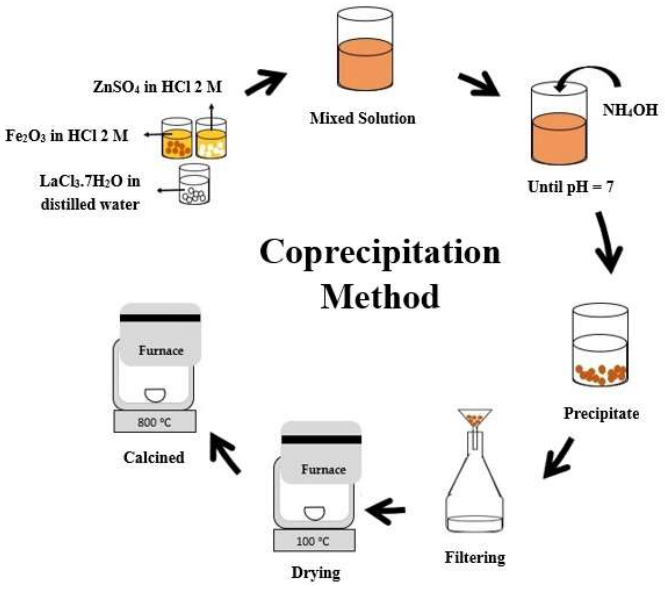

Figure 1. The synthesis processes of $LaFeO_3/Fe_2O_3$ doped with ZnO powders.

2.3. Fabrication and characterization of thick-film ceramics

Firstly, each material is produced using the synthesis process, consisting of $LaFeO_3/Fe_2O_3$, and its modification of 0.5 mol% ZnO doped, which are prepared using material paste. These processes are performed by mixing the synthesized materials and organic vehicles in a ratio of 7:3. First, the mixtures are manually stirred using a stainless micro spatula for about 2 h until they become homogeneous. The organic vehicle is then fabricated from a mixture of ethyl cellulose and alpha-terpineol in a ratio of 1:9.

Second, thick-film ceramics are fabricated using the screen-printing technique using alumina as the substrate, which has a thickness of about 0.5 mm and a size of 1.0 × 0.5 cm, as shown in Figure 2a. The process starts with printing the silver paste (Ag) as the material electrode is placed over the alumina substrates, as shown in Figure 2b, and fired at 600 ℃ for 10 min. Then, the material paste is printed over the silver coating, as shown in Figure 2c, and fired at 600 ℃ for 2 h.

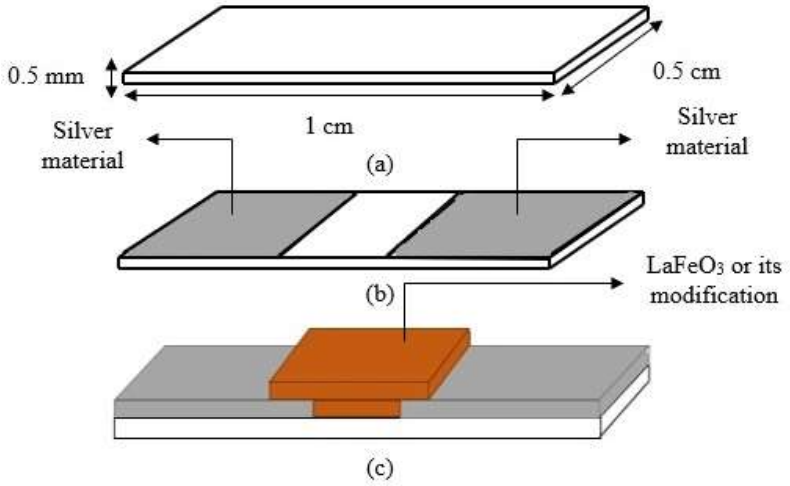

Figure 2. The flow of thick film fabrication: (a) alumina substrates, (b) silver printing, and (c) material paste printing.

The ethanol gas sensor based on thick-film ceramic $LaFeO_3/Fe_2O_3$ and its modification with 0.5 mol% ZnO were respectively characterized in terms of crystal and morphological structure using XRD and SEM. XRD characterization was performed using a PANanalytical X'Pert Pro Series PW3040/x0 X'Pert Pro with a $CuK_\alpha 1$ wavelength of 1.5404×10^{-10} m.

The XRD characterization was used to determine the average of crystallite size that was calculated using the Debye-Scherrer formula as shown in Eq 1 [37–41]. Where λ is the x-ray wavelength used in this characterization, B is the peak of full width at half-maximum (FWHM) intensity, and θ is the angle of Bragg diffraction.

$$D = \frac{0.89\,\lambda}{B\cos\theta} \tag{1}$$

SEM characterization was conducted using scanning electron microscopy analysis (JEOL JSM-6360LA). SEM was used to characterize the grain size of the materials. Further, the electrical properties were also considered to investigate the sensor's ethanol gas detection performance. The electrical properties were characterized using a static gas chamber as previously reported [32]. The

electrical properties investigated included the responses and operating temperature of the ethanol gas sensor based on $LaFeO_3$ and its modification. In this work, the samples were placed in a static gas chamber without ethanol gas as the ambient condition, with various ethanol gases conditions, i.e., 100, 200, and 300 ppm. The output of this characterization was the resistance value of the thick film that was measured at various temperatures (from room temperature up to 215 ℃) and displayed by an ohmmeter. This process determines the resistance value. Then, the resistance value was processed and calculated using Eq 2 to obtain the response of $LaFeO_3/Fe_2O_3$ and its modification with 0.5 mol% ZnO doped in ethanol detection processes [42–46]. Where R_g is the resistance of the gas sensor in ethanol gas and R_a is the resistance of the gas sensor in air (ambient condition or without ethanol gas).

$$\text{Response} = \frac{R_g}{R_a} \times 100\% \tag{2}$$

3. Results

In this research, we reported the data accomplished in the experiment. Firstly, the synthesis process was conducted to produce the materials, $LaFeO_3/Fe_2O_3$ and its modification with 0.5 mol% ZnO doped. This process produced the dark brown powders for $LaFeO_3/Fe_2O_3$ and brown light powders for 0.5 mol% ZnO doped $LaFeO_3/Fe_2O_3$. Then, both of the materials were characterized using XRD to determine their crystal characteristics within the results, as shown in Figure 3. This characterization also indicates the crystallite size and their effect on the performance of $LaFeO_3/Fe_2O_3$ and its modification with 0.5 mol% ZnO doped as ethanol gas sensing. The crystallite size is calculated using Eq 1 and produces the results in Table 1. These results show that 0.5 mol% ZnO doped decreases the crystallite size of $LaFeO_3/Fe_2O_3$.

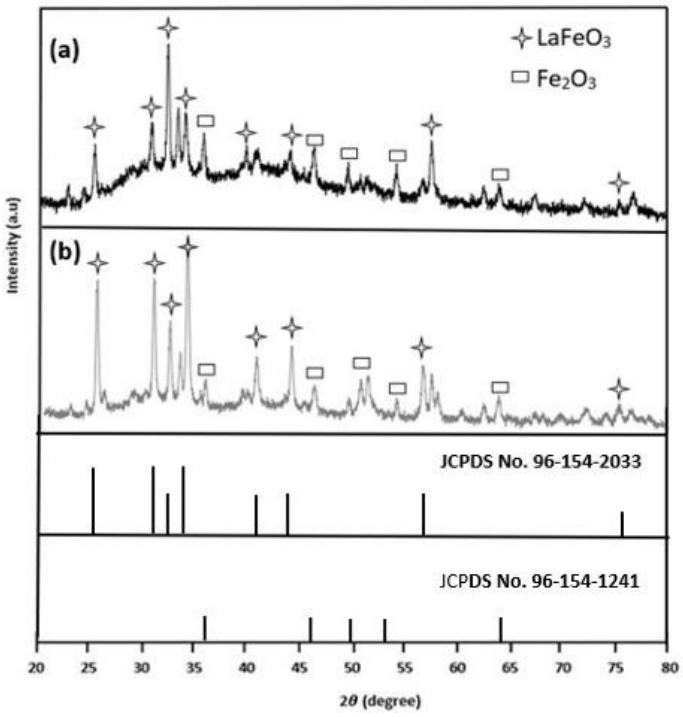

Figure 3. XRD pattern of (a) $LaFeO_3/Fe_2O_3$ and (b) its modification with 0.5 mol% ZnO doped.

Table 1. Crystal parameters of $LaFeO_3/Fe_2O_3$ and its modification with ZnO doped.

Material	Crystal structures	Lattice Parameters (Å)	Crystallite Size (nm)
$LaFeO_3$	cubic	3.8977	61.4
$LaFeO_3$/ Fe_2O_3 with 0.5 mol% ZnO	cubic	3.9516	28.8

Furthermore, the SEM characterization was also conducted to determine the morphological properties of $LaFeO_3/Fe_2O_3$ and its modification with 0.5 mol% ZnO doped. The characterization results are shown in Figure 4. These results indicate that the grain sizes of the materials are relatively similar but not uniform.

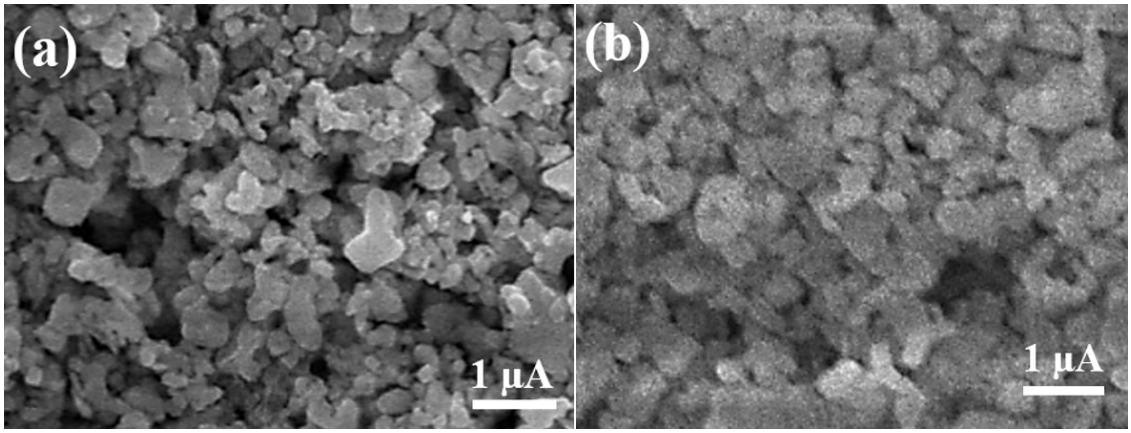

Figure 4. SEM images of (a) $LaFeO_3/Fe_2O_3$ and (b) its modification with 0.5 mol% ZnO doped.

Lastly, the electrical properties characterization was conducted to determine the performance of $LaFeO_3/Fe_2O_3$ and its modification with 0.5 mol% ZnO doped to detect the ethanol gases. This performance test was conducted by resistance measurement using an ohmmeter. First, the resistance measurement is conducted in the different concentrations of ethanol gases, i.e., with 100 ppm, 200 ppm, and 300 ppm. Then, the resistance value is graphically indicated as the temperature function, as shown in Figure 5.

As mentioned in Section 2.3, the resistance value obtained from the experiment was calculated using Eq 2 and produced the response of $LaFeO_3/Fe_2O_3$ and its modification with 0.5 mol% ZnO doped in the processes of ethanol gas detection. The response value is shown in Figure 6. The response of $LaFeO_3/Fe_2O_3$ increases from 257% to 309% at 300 ppm. Figure 6 also illustrates that the operating temperature of $LaFeO_3/Fe_2O_3$ decreases from 205 ℃ to 180 ℃, caused by the 0.5 mol% ZnO doped.

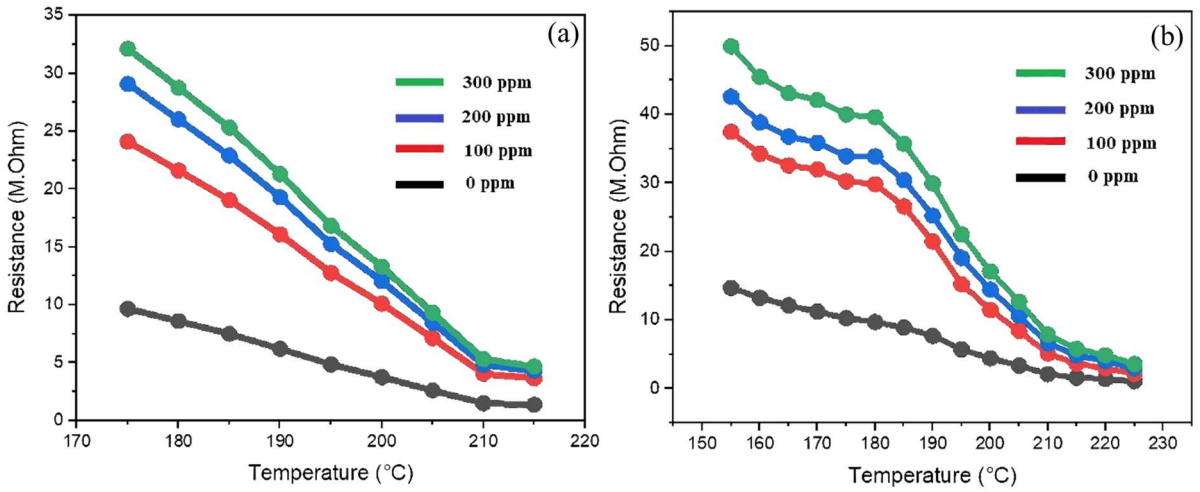

Figure 5. The resistance of (a) $LaFeO_3/Fe_2O_3$ and (b) its modification with 0.5 mol% ZnO doped in environments without ethanol and with ethanol gas at various concentrations (100, 200, and 300 ppm).

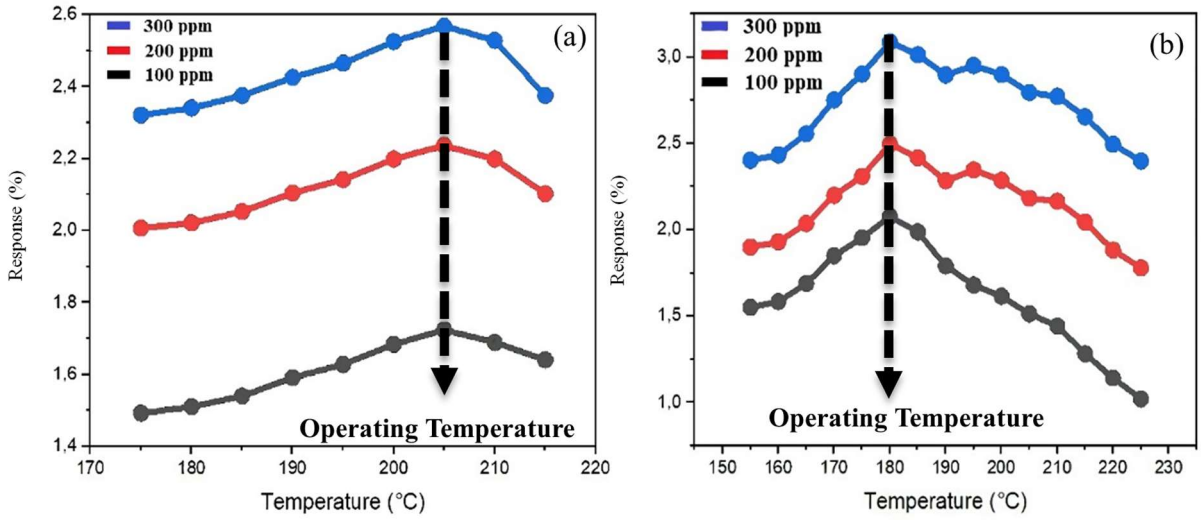

Figure 6. Ethanol response of (a) $LaFeO_3/Fe_2O_3$ and (b) its modification with 0.5 mol% ZnO doped.

4. Discussion

In this experiment, we had been successfully synthesized the $LaFeO_3/Fe_2O_3$ and its modification with 0.5 mol% ZnO doped. Then, these materials were characterized using XRD, SEM, and electrical properties.

XRD pattern shows that the materials have two phases, i.e., $LaFeO_3$ and Fe_2O_3, and it has been fitted with the JCPDS No. 96-154-2033 for $LaFeO_3$ and JCPDS No. 96-101-1241 for Fe_2O_3. The JCPDS number were known from the analysis process using Match 3. However, there are still other peaks in the XRD pattern, possibly caused by the impurities of yarosite minerals shown in Table 2. The impurities of the yarosite mineral have been reported by Ariyani et al. [47].

Table 2. The compounds contained in the yarosite mineral used in this research.

No.	Compound	wt%
1	Fe_2O_3	91.30
2	Al_2O_3	3.30
3	SiO_2	2.05
4	TiO_2	3.02
5	CaO	0.16
6	MnO	0.17

The XRD data also inform the crystallite size, as shown in Table 1. This experiment shows that the crystallite size decreases drastically after 0.5 mol % zinc oxide is added into $LaFeO_3/Fe_2O_3$. The crystallite size affects the response of a gas sensor. The smaller the crystallite size, the better the response of the gas sensor [48]. Apart from that, the other characterization conducted in this experiment is SEM. This characterization informed that 0.5 mol% ZnO doped influences the morphological structure of $LaFeO_3/Fe_2O_3$. Based on Figure 4, it is found that the 0.5 mol% ZnO doped also decreases the grain size of $LaFeO_3/Fe_2O_3$, and it has an effect on the materials' performance in the detecting the target, which in this research is ethanol gases.

The performance test starts with the resistance measurement of both materials, $LaFeO_3/Fe_2O_3$ and its modification of 0.5 mol% ZnO doped. This process produces the graphic of resistance function to the temperature, as shown in Figure 5. It informs that the resistance increases as the ethanol gas concentration increases, confirming that $LaFeO_3/Fe_2O_3$ and its modification with 0.5 mol% ZnO doped are p-type semiconductors [49]. This is strengthened by the claim that the p-type semiconductor of the gas sensor has a greater resistance in the ethanol contained solution compared to in the ambient condition [50].

Then, the resistance is calculated using Eq 2 to produce the value of the gas sensor response of $LaFeO_3/Fe_2O_3$ and its modification, as shown in Figure 6. The results show that the response of the gas sensor is affected by the concentration of ethanol gas. In addition, the dopant also strongly affects the gas response, with is similar to the result reported by Gao et al. [51].

In this research, as explained in the previous section, the response of $LaFeO_3/Fe_2O_3$ increases when 0.5 mol% zinc oxide is added. The modification of $LaFeO_3/Fe_2O_3$ with 0.5 mol% zinc oxide produces a suitable gas-sensing material. It is known from the compares results of this study with the other studies of $LaFeO_3$ or Fe_2O_3 that have been applied as ethanol gas sensors with the addition of doping as listed in Table 3. From the Table 3 were known that the type of doping was influence the response value of $LaFeO_3$ or Fe_2O_3. It caused by the different characteristics of the doping. The doping can help the $LaFeO_3$ or Fe_2O_3 to bind the oxygen atoms that contains in ethanol gases [52]. Therefore, Suhendi et al. [32] reported that using co-doping has a higher response than this work.

The addition of 0.5 mol% zinc oxide also decreases the operating temperature of $LaFeO_3/Fe_2O_3$, indicating that zinc oxide doping improves the characteristics of $LaFeO_3/Fe_2O_3$ as a gas-sensing material. The reduce operating temperature of undoped and 0.5 mol% zinc oxide doped $LaFeO_3/Fe_2O_3$ were caused by the different activation and adsorbing energies from both materials [53]. The mechanism was described by the $LaFeO_3$ sensing processes that occurred as a result of the interaction between absorbed gas molecules in the surface of the gas sensor that change the conductivity [54]. Nonetheless, the main reason of zinc oxide doping could be reducing the operating temperature for $LaFeO_3/Fe_2O_3$ is zinc oxide has high reactivity and easy adsorption of oxygen atoms which is

contained in ethanol, its characteristics were help $LaFeO_3/Fe_2O_3$ to capture ethanol gases molecules around the surface [52].

Table 3. A comparison of the ethanol gas sensing response and operating temperature of $LaFeO_3$ doped with different elements.

Elements doping	Concentration (ppm)	Response	Operating temperature (°C)	Ref
Zn	300	3.09	180	This work
Co-doped Ca and Zn	300	3.65	190	[32]
Sr	300	3.05	300	[37]

The sensing mechanism through which $LaFeO_3/Fe_2O_3$ and its modification detect ethanol gases is explained by the adsorption and desorption of gas molecules on the surface of the thick film. When the surface of the thick film is exposed to air (without ethanol gases), the oxygen molecules are absorbed by the material's surface to produce chemisorbed oxygen. The chemisorbed oxygen catches the electrons of the conduction band (CB). These processes can be explained by the reaction shown in Eqs 3–5 [55–57].

$$O_2\ (gas) \leftrightarrow O_2\ (ads) \tag{3}$$

$$O_2\ (ads) + e^-\ (CB) \leftrightarrow O_2^-\ (ads) \tag{4}$$

$$O_2^-\ (ads) + e^-\ (CB) \leftrightarrow 2O^-\ (ads) \tag{5}$$

When the thick-film surface is exposed to ethanol, the adsorbed oxygen reacts with ethanol by releasing the trapped electrons to the gas-sensing material, in this case, $LaFeO_3/Fe_2O_3$ and its modification. These processes cause the resistance of the gas-sensing material to increase when it is exposed to ethanol gas, as shown in Figure 5. The interaction of adsorbed oxygen and ethanol can be explained in the reaction shown in Eq 6 [58].

$$C_2H_5OH\ (gas) + 6O^- \leftrightarrow 2CO_2 + 3H_2O + 6e^- \tag{6}$$

5. Conclusions

In summary, ethanol gas sensors based on $LaFeO_3/Fe_2O_3$ doped with 0.5 mol% zinc-oxide-based thick-film ceramics were produced using a screen-printing technique. We also used yarosite minerals as the Fe_2O_3 precursor to Indonesia's natural resources. The performance of the gas sensors was investigated using three types of characterizations, i.e., XRD to determine the crystal structure, SEM to determine the morphological structure, and electrical properties to determine the ability of the materials to detect ethanol gas. These characterizations show that yarosite minerals have the potential to be applied in ethanol gas sensors. ZnO doping reduces the crystallite size and grain size of $LaFeO_3/Fe_2O_3$, causes the materials to bind the targets more easily and improves the response of ethanol gas sensors. Importantly, ZnO doping increases the response of $LaFeO_3/Fe_2O_3$ to detect ethanol gases from about 257% to 309%. Lastly, the use of yarosite minerals reduces the cost of the fabrication process. Overall, the results show that doping plays an important role in improving the performance of gas-sensing materials; $LaFeO_3/Fe_2O_3$ and yarosite minerals can be further explored to improve ethanol gas sensing in the future.

Acknowledgments

This work was financially supported by "Hibah Penelitian Terapan Unggulan Perguruan Tinggi Kementerian Pendidikan, Kebudayaan, Riset, dan Teknologi Republik Indonesia" research grants for the 2020 fiscal year.

Conflict of interest

The authors declare no conflict of interest.

References

1. Zhang X, Lan W, Xu J, et al. (2019) ZIF-8 derived hierarchical hollow ZnO nanocages with quantum dots for sensitive ethanol gas detection. *Sens Actuators B Chem* 289: 144–152. https://doi.org/10.1016/j.snb.2019.03.090
2. Wang C, Wang ZG, Xi R, et al. (2019) In situ synthesis of flower-like ZnO on GaN using electrodeposition and its application as ethanol gas sensor at room temperature. *Sens Actuators B Chem* 292: 270–276. https://doi.org/10.1016/j.snb.2019.04.140
3. Zhang S, Wang C, Qu F, et al. (2019) ZnO nanoflowers modified with RuO_2 for enhancing acetone sensing performance. *Nanotechnology* 31: 115502. https://doi.org/10.1088/1361-6528/ab5cd9
4. Wang X, Liu F, Chen X, et al. (2020) SnO_2 core-shell hollow microspheres co-modification with Au and NiO nanoparticles for acetone sensing. *Powder Technol* 364: 159–166. https://doi.org/10.1016/j.powtec.2020.02.006
5. Yin M, Wang Y, Yu L, et al. (2020) Ag nanoparticles-modified Fe_2O_3@MoS_2 core-shell micro/nanocomposites for high-performance NO_2 gas detection at low temperature. *J Alloys Compd* 829: 153371. https://doi.org/10.1016/j.jallcom.2020.154471
6. Tan J, Hu J, Ren J, et al. (2020) Fast response speed of mechanically exfoliated MoS_2 modified by PbS in detecting NO_2. *Chinese Chem Lett* 31: 2103–2108. https://doi.org/10.1016/j.cclet.2020.03.060
7. Luo N, Zhang D, Xu J (2020) Enhanced CO sensing properties of Pd modified ZnO porous nanosheets. *Chinese Chem Lett* 31: 2033–2036. https://doi.org/10.1016/j.cclet.2020.01.002
8. Zhu K, Ma S, Tie Y, et al. (2019) Highly sensitive formaldehyde gas sensors based on Y-doped SnO_2 hierarchical flower-shaped nanostructures. *J Alloys Compd* 792: 938–944. https://doi.org/10.1016/j.jallcom.2019.04.102
9. Cao J, Wang S, Zhao X, et al. (2020) Facile synthesis and enhanced toluene gas sensing performances of Co_3O_4 hollow nanosheets. *Mater Lett* 263: 127215. https://doi.org/10.1016/j.matlet.2019.127215
10. Zhang C, Luo Y, Xu J, et al. (2019) Room temperature conductive type metal oxide semiconductor gas sensors for NO_2 detection. *Sens Actuator A Phys* 289: 118–133. https://doi.org/10.1016/j.sna.2019.02.027
11. Liu W, Xie Y, Chen T, et al. (2019) Rationally designed mesoporous In_2O_3 nanofibers functionalized Pt catalyst for high-performance acetone gas sensors. *Sens Actuators B Chem* 298: 126871. https://doi.org/10.1016/j.snb.2019.126871

12. Song Z, Zhang J, Jiang J (2020) Morphological evolution, luminescence properties and a high-sensitivity ethanol gas sensor based on 3D flower-like MoS_2-ZnO micro/nanosphere arrays *Ceram Int* 46: 6634–6640. https://doi.org/10.1016/j.ceramint.2019.11.151
13. Zhang K, Qin S, Tang P, et al. (2020) Ultra-sensitive ethanol gas sensors based on nanosheet-assembled hierarchical ZnO-In_2O_3 heterostructures. *J Hazard Mater* 391: 122191. https://doi.org/10.1016/j.jhazmat.2020.122191
14. Cao P, Yang Z, Navale ST, et al. (2019) Ethanol sensing behavior of Pd-nanoparticles decorated ZnO-nanorod based chemiresistive gas sensors. *Sensor Actuat B Chem* 298: 126850. https://doi.org/10.1016/j.snb.2019.126850
15. Zeng Q, Cui Y, Zhu L, et al. (2020) Increasing oxygen vacancies at room temperature in SnO_2 for enhancing ethanol gas sensing. *Mat Sci Semicon Proc* 111: 104962. https://doi.org/10.1016/j.mssp.2020.104962
16. Yu HL, Wang J, Zheng B, et al. (2020) Fabrication of single crystalline WO_3 nano-belts based photoelectric gas sensor for detection of high concentration ethanol gas at room temperature. *Sens Actuator A Phys* 303: 111865. https://doi.org/10.1016/j.sna.2020.111865
17. Mao JN, Hong B, Chen HD, et al. (2020) Highly improved ethanol gas response of n-type α-Fe_2O_3 bunched nanowires sensor with high-valence donor-doping. *J Alloys Compd* 827: 154248. https://doi.org/10.1016/j.jallcom.2020.154248
18. Cao E, Wu A, Wang H, et al. (2019) Enhanced ethanol sensing performance of Au and Cl comodified $LaFeO_3$ nanoparticles. *ACS Appl Nano Mater* 2: 1541–1551. https://doi.org/10.1021/acsanm.9b00024
19. Shingange K, Swart HC, Mhlongo, GH (2020) Design of porous p-type $LaCoO_3$ nanofibers with remarkable response and selectivity to ethanol at low operating temperature. *Sensor Actuat B Chem* 308: 127670. https://doi.org/10.1016/j.snb.2020.127670
20. Cao E, Feng Y, Guo Z, et al. (2020) Ethanol sensing characteristics of (La,Ba)(Fe,Ti)O_3 nanoparticles with impurity phases of $BaTiO_3$ and $BaCO_3$. *J Sol-Gel Sci Techn* 96: 431–440. https://doi.org/10.1007/s10971-020-05369-x
21. Xiang J, Chen X, Zhang X, et al. (2018) Preparation and characterization of Ba-doped $LaFeO_3$ nanofibers by electrospinning and their ethanol sensing properties. *Mater Chem Phys* 213: 122–129. https://doi.org/10.1016/j.matchemphys.2018.04.024
22. Nga PTT, My DTT, Duc NM, et al. (2021) Characteristics of porous spherical $LaFeO_3$ as ammonia gas sensing material. *Vietnam J Chem* 59: 676–683.
23. Zhang Y, Zhao J, Sun H, et al. (2018) B, N, S, Cl doped graphene quantum dots and their effect on gas-sensing properties of Ag-$LaFeO_3$. *Sensor Actuat B Chem* 266: 364–374. https://doi.org/10.1016/j.snb.2018.03.109
24. Zhang W, Yang B, Liu J, et al. (2017) Highly sensitive and low operating temperature SnO_2 gas sensor doped by Cu and Zn two elements. *Sensor Actuat B Chem* 243: 982–989. https://doi.org/10.1016/j.snb.2016.12.095
25. Qin J, Cui Z, Yang X, et al. (2015) Three-dimensionally ordered macroporous $La_{1-x}Mg_xFeO_3$ as high performance gas sensor to methanol. *J Alloys Compd* 635: 194–202. https://doi.org/10.1016/j.jallcom.2015.01.226
26. Chen M, Wang H, Hu J, et al. (2018) Near-room-temperature ethanol gas sensor based on mesoporous Ag/Zn-$LaFeO_3$ nanocomposite. *Adv Mater Interfaces* 6: 1801453. https://doi.org/10.1002/admi.201801453

27. Wang C, Rong Q, Zhang Y, et al. (2019) Molecular imprinting Ag-$LaFeO_3$ spheres for highly sensitive acetone gas detection. *Mater Res Bull* 109: 265–272. https://doi.org/10.1016/j.materresbull.2018.09.040
28. Koli PB, Kapadnis KH, Deshpande UG, et al. (2020) Sol-gel fabricated transition metal Cr^{3+}, Co^{2+} doped lanthanum ferric oxide (LFO-$LaFeO_3$) thin film sensors for the detection of toxic, flammable gases: A comparative study. *Mat Sci Res India* 17: 70–83. https://doi.org/10.13005/msri/170110
29. Ma L, Ma SY, Qiang Z, et al. (2017) Preparation of Co-doped $LaFeO_3$ nanofibers with enhanced acetic acid sensing properties. *Mater Lett* 200: 47–50. https://doi.org/10.1016/j.matlet.2017.04.096
30. Manzoor S, Husain S, Somvanshi A, et al. (2019) Impurity induced dielectric relaxor behavior in Zn doped $LaFeO_3$. *J Mater Sci Mater Electron* 30: 19227–19238. https://doi.org/10.1007/s10854-019-02281-1
31. Tumberphale UB, Jadhav SS, Raut SD, et al. (2020) Tailoring ammonia gas sensing performance of La^{3+}-doped copper cadmium ferrite nanostructures. *Solid State Sci* 100: 106089. https://doi.org/10.1016/j.solidstatesciences.2019.106089
32. Suhendi E, Amanda ZA, Ulhakim MT, et al. (2021) The enhancement of ethanol gas sensors response based on calcium and zinc co-doped $LaFeO_3$/Fe_2O_3 thick film ceramics utilizing yarosite minerals extraction as Fe_2O_3 precursor. *J Met Mater Miner* 31: 71–77.
33. Lai T, Fang T, Hsiao Y, et al (2019) Characteristics of Au-doped SnO_2-ZnO heteronanostructures for gas sensing applications. *Vacuum* 166: 155–161. https://doi.org/10.1016/j.vacuum.2019.04.061
34. Ehsani M, Hamidon MN, Toudeshki A, et al. (2016) CO_2 gas sensing properties of screen-printed La_2O_3/SnO_2 thick film. *IEEE Sens J* 16: 6839–6845. https://doi.org/10.1109/JSEN.2016.2587779
35. Isabel RTM, Onuma S, Angkana P, et al. (2018) Printed PZT thick films implemented for functionalized gas sensors. *Key Eng Mater* 777: 158–162. https://doi.org/10.4028/www.scientific.net/KEM.777.158
36. Moschos A, Syrovy T, Syrova L, et al. (2017) A screen-printed flexible flow sensor. *Meas Sci Technol* 28: 055105. https://doi.org/10.1088/1361-6501/aa5fa0
37. Suhendi E, Ulhakim MT, Setiawan A, et al. (2019) The effect of SrO doping on $LaFeO_3$ using yarosite extraction based ethanol gas sensors performance fabricated by coprecipitation method. *Int J Nanoelectron Mater* 12: 185–192.
38. Kou X, Wang C, Ding M, et al. (2016) Synthesis of Co-doped SnO_2 nanofibers and their enhanced gas-sensing properties. *Sensor Actuat B Chem* 236: 425–432. https://doi.org/10.1016/j.snb.2016.06.006
39. Wang H, Wei S, Zhang F, et al. (2017) Sea urchin-like SnO_2/Fe_2O_3 microspheres for an ethanol gas sensor with high sensitivity and fast response/recovery. *J Mater Sci Mater Electron* 28: 9969–9973. https://doi.org/10.1007/s10854-017-6755-3
40. Li Z, Yi J (2017) Enhanced ethanol sensing of Ni-doped SnO_2 hollow spheres synthesized by a one-pot hydrothermal method. *Sensor Actuat B Chem* 243: 96–103. https://doi.org/10.1016/j.snb.2016.11.136
41. Cheng Y, Guo H, Wang Y, et al. (2018) Low cost fabrication of highly sensitive ethanol sensor based on Pd-doped α-Fe_2O_3 porous nanotubes. *Mater Res Bull* 105: 21–27. https://doi.org/10.1016/j.materresbull.2018.04.025

42. Zhang J, Liu L, Sun C, et al. (2020) Sr-doped α-Fe_2O_3 3D layered microflowers have high sensitivity and fast response to ethanol gas at low temperature. *Chem Phys Lett* 750: 137495. https://doi.org/10.1016/j.cplett.2020.137495
43. Wei W, Guo S, Chen C, et al. (2017) High sensitive and fast formaldehyde gas sensor based on Ag-doped $LaFeO_3$ nanofibers. *J Alloys Compd* 695: 1122–1127. https://doi.org/10.1016/j.jallcom.2016.10.238
44. Cao E, Yang Y, Cui T, et al. (2017) Effect of synthesis route on electrical and ethanol sensing characteristics for $LaFeO_{3-\delta}$ nanoparticles by citric sol-gel method. *Appl Surf Sci* 393: 134–143. https://doi.org/10.1016/j.apsusc.2016.10.013
45. Cao E, Wang H, Wang X, et al. (2017) Enhanced ethanol sensing performance for chlorine doped nanocrystalline $LaFeO_{3-\delta}$ powders by citric sol-gel method. *Sensor Actuat B Chem* 251: 885–893. https://doi.org/10.1016/j.snb.2017.05.153
46. Zhang Y, Duan Z, Zou H, et al. (2018) Fabrication of electrospun $LaFeO_3$ nanotubes via annealing technique for fast ethanol detection. *Mater Lett* 215: 58–61. https://doi.org/10.1016/j.matlet.2017.12.062
47. Ariyani NI, Syarif DG, Suhendi E (2017) Fabrication and characterization of thick film ceramics $La_{0.9}Ca_{0.1}FeO_3$ for ethanol gas sensor using extraction of Fe_2O_3 from yarosite mineral. *IOP Conf Ser Mater Sci Eng* 384: 012037. https://doi.org/10.1088/1757-899X/384/1/012037
48. Zhou Q, Chen W, Xu L, et al. (2018) Highly sensitive carbon monoxide (CO) gas sensors based on Ni and Zn doped SnO_2 nanomaterials. *Ceram Int* 44: 4392–4399. https://doi.org/10.1016/j.ceramint.2017.12.038
49. Hao P, Qiu G, Song P, et al. (2020) Construction of porous $LaFeO_3$ microspheres decorated with NiO nanosheets for high response ethanol gas sensors. *Appl Surf Sci* 515: 146025. https://doi.org/10.1016/j.apsusc.2020.146025
50. Srinivasan P, Ezhilan M, Kulandaisamy AJ, et al. (2019) Room temperature chemiresistive gas sensors: challenges and strategies–a mini review. *J Mater Sci Mater Electron* 30: 15852–15847. https://doi.org/10.1007/s10854-019-02025-1
51. Gao H, Wei D, Lin P, et al. (2017) The design of excellent xylene gas sensor using Sn-doped NiO hierarchical nanostructure. *Sensor Actuat B Chem* 253: 1152–1162. https://doi.org/10.1016/j.snb.2017.06.177
52. Hu X, Zhu Z, Chen C, et al. (2017) Highly sensitive H_2S gas sensors based on Pd-doped CuO nanoflowers with low operating temperature. *Sensors Actuat B Chem* 253: 809–817. https://doi.org/10.1016/j.snb.2017.06.183
53. Singh G, Virpal, Singh RC (2019) Highly sensitive gas sensor based on Er-doped SnO_2 nanostructures and its temperature dependent selectivity towards hydrogen and ethanol. *Sensor Actuat B Chem* 282: 373–383. https://doi.org/10.1016/j.snb.2018.11.086
54. Phan TTN, Dinh TTM, Nguyen MD, et al. (2022) Hierarchically structured $LaFeO_3$ with hollow core and porous shell as efficient sensing material for ethanol detection. *Sensor Actuat B Chem* 354: 131195. https://doi.org/10.1016/j.snb.2021.131195
55. Montazeri A, Jamali-Sheini F (2017) Enhanced ethanol gas-sensing performance of Pb-doped In_2O_3 nanosructures prepared by sonochemical method. *Sensor Actuat B Chem* 242: 778–791. https://doi.org/10.1016/j.snb.2016.09.181
56. Mirzael A, Lee J, Majhi SM, et al. (2019) Resistive gas sensors based on metal-oxide nanowires. *J Appl Phys* 126: 241102. https://doi.org/10.1063/1.5118805

57. Yang K, Ma J, Qiao X, et al. (2020) Hierarchical porous $LaFeO_3$ nanostructure for efficient trace detection of formaldehyde. *Sensor Actuat B Chem* 313: 128022. https://doi.org/10.1016/j.snb.2020.128022
58. Liu C, Navale ST, Yang ZB, et al. (2017) Ethanol gas-sensing properties of hydrothermally grown α-MnO_2 nanorods. *J Alloys Compd* 727: 362–369. https://doi.org/10.1016/j.jallcom.2017.08.150

AIMS Press